Electronic Supplementary Information for

Tunable Valley and Spin Splitting in 2*H*-VSe_2/$BiFeO_3$(111) Triferroic Heterostructures

Fang Zhang,[a] Wenbo Mi*,[a] and Xiaocha Wang*,[b]

[a]*Tianjin Key Laboratory of Low Dimensional Materials Physics and Preparation Technology, School of Science, Tianjin University, Tianjin 300354, China*

[b]*Tianjin Key Laboratory of Film Electronic & Communicate Devices, School of Electronics Information Engineering, Tianjin University of Technology, Tianjin 300384, China*

*Author to whom all correspondence should be addressed.

E-mail: miwenbo@tju.edu.cn and wangxc@email.tjut.edu.cn

Table S1 Magnetic moment of pristine $\sqrt{3}\times\sqrt{3}$ VSe_2 monolayer, magnetic moment (M_{VSe_2}) of VSe_2 monolayer in VSe_2/BFO heterostructures, and the total magnetic moment (M_{total}) of 2*H*-VSe_2/BFO(111) heterostructures.

Model	Pristine VSe_2	Fe_{up}	Fe_{dn}	Bi_{up}	Bi_{dn}	$Fe(Se)_{up}$	$Fe(+)_{up}$
M_{VSe_2} (μ_B)	2.93	-0.10	-2.10	-0.01	-0.02	-2.61	2.74
M_{total} (μ_B)	-	-3.80	-4.86	0.94	-0.80	-6.80	7.39

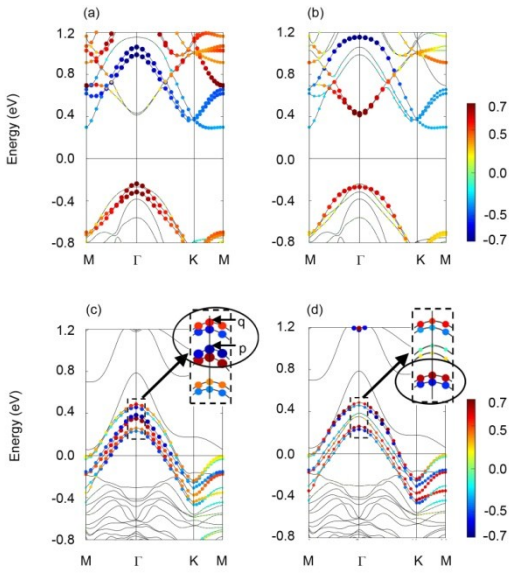

Fig. S1. The band structure of $\sqrt{3}\times\sqrt{3}$ VSe_2 (upper) and Fe_{up} model (lower). The marking parts in (a) and (c) represent the contribution of V d_{xy} and $d_{x^2-y^2}$ orbitals. The marking parts in (b) and (d) represent the contribution of V d_{z^2} orbital. The inset in (c) and (d) show an enlarged top of valence band at Γ point.

According to the size and color of the circle and the shape of the bands in Figs. S1(c) and (d), the origin of six bands from 0.0 eV to 0.5 eV at the Γ point in Fe_{up} can be known. The highest and second highest bands carry a pair of spin-up and spin-down polarized states (group 1), and the third and fourth highest bands carry another pair of spin-up and spin-down polarized states (group 2). In Fig. S1(c), group 1 and group 2 hold large and dark-colored circles. In Fig. S1(d), the two bands with the lowest energy (group 3) hold large and dark-colored circles. Hence, group 1 and 2 come from respectively the different $K_{\pm}$ points, and group 3 originate from Γ point.

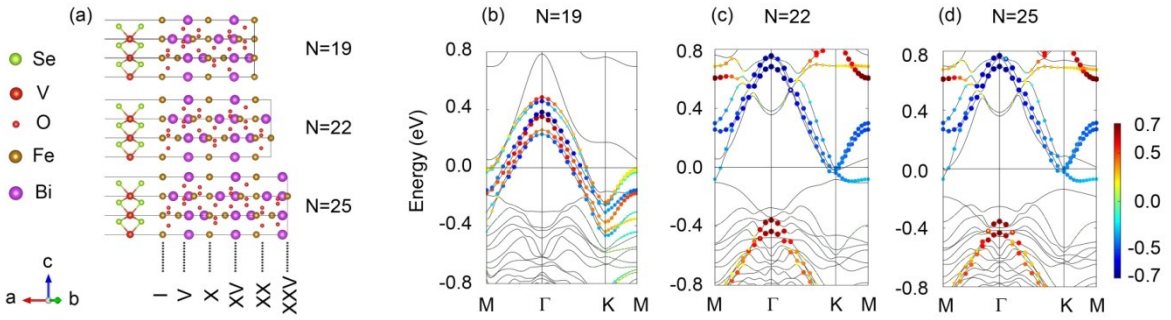

Fig S2. (a) Atomic structure for 2*H*-VSe_2/BFO(111) heterostructures with different atomic layers of BFO substrate (*N*=19, 22 and 25). (b-d) Components of VSe_2 in band structure for 2H-VSe_2/BFO(111) heterostructures with SOC calculations.

The models whose BFO substrate with 22 and 25 atomic layer thicknesses are tested (*N*=22/25), which have the same stacking pattern as the Fe_{up} (*N*=19). The geometry and band structures of these models are shown in Fig. S2. The valley and spin splitting energies at Γ point in the models with *N*=22/25 (Table S2) are close to that of pristine monolayer VSe_2 (ΔV = 78.23 meV and ΔE = 1.18 eV). While, the valley splitting energy increased to 101.92 meV and spin splitting energy decreased to 0.03 eV in the model with *N*=19. Hence, the spin and valley splitting of monolayer VSe_2 are more obviously modulated in the heterostructures when the thickness of the BFO substrate is 19 atomic layers.

Table S2 Valley splitting energy (ΔV) and spin splitting energy (ΔE) of 2*H*-VSe_2/BFO(111) heterostructures with different thicknesses of BFO substrate (*N*=19, 22 and 25).

N (atoms layer)	19	22	25
ΔV (meV)	101.92	80.54	77.26
ΔE (eV)	0.03	1.04	1.05

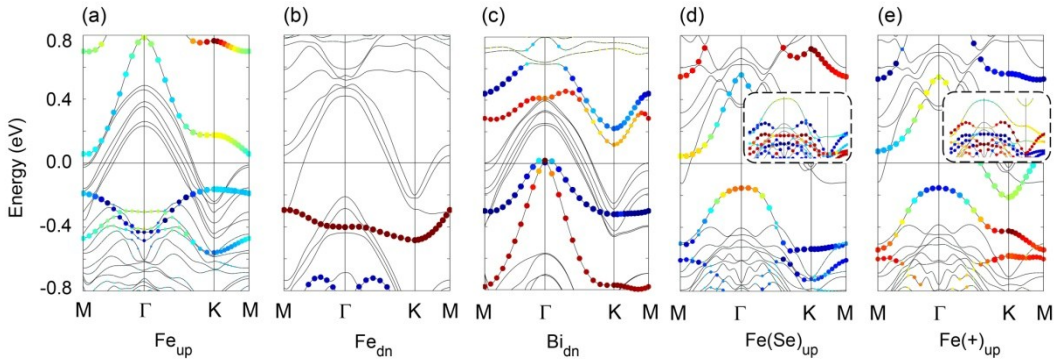

Fig. S3 Atomic-resolved band structure of the Fe_{up}, Fe_{dn}, Bi_{dn}, $Fe(Se)_{up}$ and $Fe(+)_{up}$. The marking parts represent the contribution of O, Fe and Bi atoms below XVII atomic layer of the BFO substrate in each model. The inset in (d) and (e) are the contribution of all O atom in the substrate.

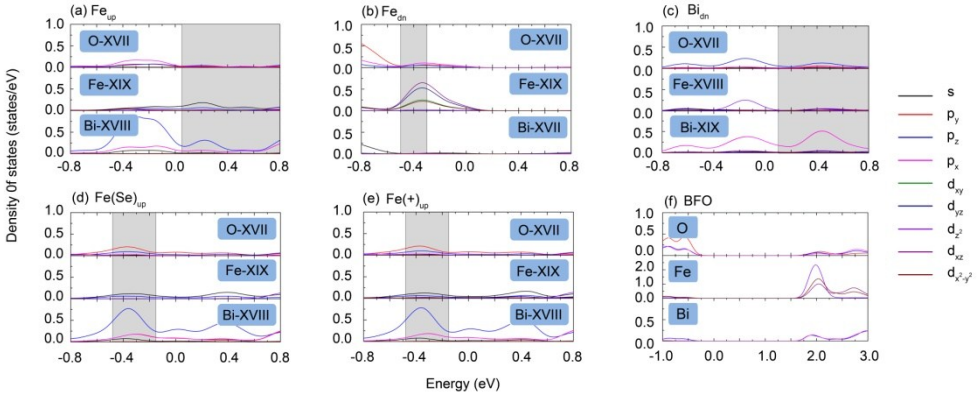

Fig. S4 Orbital-resolved density of states of (DOS) the bottom atoms in (a) Fe_{up}, (b) Fe_{dn}, (c) Bi_{dn}, (d) $Fe(Se)_{up}$, (e) $Fe(+)_{up}$, and DOS of the O, Fe and Bi atoms in bulk BFO. Shadow area is the energy range of the unconcerned bands.